Defense Technical Information Center
Compilation Part Notice

ADP013664

TITLE: Large Eddy and Detached Eddy Simulations Using an Unstructured Multigrid Solver

DISTRIBUTION: Approved for public release, distribution unlimited

This paper is part of the following report:

TITLE: DNS/LES Progress and Challenges. Proceedings of the Third AFOSR International Conference on DNS/LES

To order the complete compilation report, use: ADA412801

The component part is provided here to allow users access to individually authored sections of proceedings, annals, symposia, etc. However, the component should be considered within the context of the overall compilation report and not as a stand-alone technical report.

The following component part numbers comprise the compilation report:
ADP013620 thru ADP013707

LARGE EDDY AND DETACHED EDDY SIMULATIONS USING AN UNSTRUCTURED MULTIGRID SOLVER

DIMITRI J. MAVRIPLIS
ICASE
NASA Langley Research Center, Hampton, VA, USA

JUAN PELAEZ
Department of Aerospace Engineering
Old Dominion University, Norfolk, VA, USA

AND

OSAMA KANDIL
Department of Aerospace Engineering
Old Dominion University, Norfolk, VA, USA

1. Introduction

This work is concerned with the development of an efficient parallel Large Eddy Simulation (LES) and Detached Eddy Simulation (DES) capability using unstructured meshes. The advantages of unstructured meshes include flexible modeling of complex geometries, adaptive meshing capabilities, and homogeneous data structures well suited for massively parallel computer architectures. On the other hand, unstructured mesh techniques require additional computer resources as compared to cartesian or structured mesh methods, and the achievable accuracy of the particular unstructured mesh discretization must be carefully considered. The approach developed in this work is based on an existing steady-state unstructured mesh solver which relies on agglomeration multigrid for rapid convergence and has been shown to scale well on inexpensive personal computer (PC) clusters as well as on massively parallel supercomputers using thousands of processors [1]. A vertex-based discretization is used, where the flow variables are stored at the vertices of the mesh, and a single edge-based data structure capable of handling combinations of tetrahedra, hexahedra, prism and pyramids is employed. Spatial discretization is achieved through a central-difference control-volume formulation with scaled matrix-based artificial dissipation

461

derived from an upwind Roe-Rieman solver. This discretization is second-order accurate in space. The baseline steady-state solver is extended to an unsteady Reynolds-Averaged Navier-Stokes (URANS) solver, using a second-order accurate three-point backwards difference time discretization [2]. At each physical time-step, the parallel agglomeration multigrid algorithm is employed to drive the non-linear (unsteady) residual to convergence. The agglomeration algorithm automatically constructs coarse levels in a pre-processing phase, based on the graph of the original fine grid. A preconditioned multi-stage iterative scheme is then used on each grid level to drive the multigrid algorithm. Jacobi (point-wise) preconditioning is used in isotropic regions of the grid, while line preconditioning is used in highly stretched regions of the grid such as near walls where high grid stretching is required to resolve thin boundary layers [3]. The steady and unsteady RANS solver employs the one equation turbulence model of Spalart and Allmaras [4]. The extension from RANS to LES and DES is achieved through the modification of the length scale definition d in the Spalart-Allmaras turbulence model. In the original model, d is taken as the distance at a given grid point to the closest wall. In the DES extension proposed by Spalart [5], this length scale is replaced by:

$$d_{DES} = min(d, C_{DES}, \Delta x) \qquad (1)$$

where d represents the original closest-wall length scale, C_{DES} represents a model constant taken as 0.65, and Δx represents a measure of the local grid spacing. For unstructured meshes, Δx is taken as the maximum edge length touching a given vertex. In regions far removed from walls, this modification to the turbulence model emulates a simple Smagorinsky model for LES, while reverting in a smooth manner to the well-established Spalart-Allmaras RANS model in near wall boundary-layer regions.

The resulting solution methodology is nominally second-order accurate in space and in time. We avoid the construction of higher-order accurate spatial operators in order to be able to retain all the discretization, solution, and parallelization techniques previously developed in the steady-state solver context. However, extra care must be taken to avoid excessive numerical diffusion from the second-order discretization from dominating the turbulence eddy viscosity levels in LES regions. With this in mind, the individual convective and numerical dissipative terms of the discretization are evaluated separately, and a (constant) scaling factor is applied to the dissipative terms which provides the option for reducing these terms from their nominal values obtained when the scheme is written as an upwind Roe-Rieman solver.

The agglomeration multigrid algorithm, which is used here as a non-linear implicit solver in time, removes any stability restrictions on the per-

missible time-step size, thus allowing the time-step choice to be determined solely by accuracy considerations. While the desirable time-step size in LES regions may be small enough to obviate the need for a fully implicit solver, in the DES mode very high Courant numbers will almost always be encountered in boundary layer regions, where the solver reverts to a RANS behavior, thus making the availability of an implicit solver essential.

In the following sections, the solver is validated first in unsteady RANS mode for the flow over a circular cylinder. Validation in the LES regime is then undertaken by computing the decay of isotropic turbulence in a periodic box. Finally, the flow over a sphere is simulated in DES mode and compared with experiment and with an equivalent simulation using the solver in an unsteady RANS mode.

2. Unsteady RANS Flow Over a Circular Cylinder

The flow around a circular cylinder is a well- known case, which has been widely studied computationally and experimentally. This case is used as the basis for validation of the unsteady RANS solver, and for assessing grid resolution and time-step requirements for accurately predicting the vortex shedding frequency observed in the cylinder flow. Two different meshes of 252,000 and 631,000 grid points and three different time-steps of 0.5, 0.25 and 0.1 were used. The time-step is non-dimensionalized as $t = t_o U_{inf}/d$ where d is diameter of the cylinder and U_{inf} is the freestream velocity.

The one equation Spalart-Allmaras turbulence model [4] was used for all calculations in fully turbulent mode. In all cases the agglomeration multigrid strategy was used with four levels. The Mach number is 0.2 and the Reynolds number is 1200 for this case. All runs were performed in parallel using 16 processors of an Intel 500 MHz Pentium III PC cluster.

The computational domain in the plane normal to the cylinder span has an aspect ratio of 1 and a side length of 100 cylinder diameters. A span of two cylinder diameters is employed, and inviscid (slip velocity) boundary conditions are applied at the end-walls.

Table 1 shows the Strouhal Numbers computed for each mesh and each time-step of the cylinder flow simulations. Convergence is achieved as the time-step is reduced and the mesh size increased. A second-order accurate convergence behavior is observed as the time-step is reduced, validating the accuracy of the three-point backwards difference scheme used to discretize the time-step. From the smallest time step results, the solution can be seen to be grid converged, at least with respect to the prediction of the vortex shedding frequency. The computed Strouhal number compares very well to the experimental value of St = 0.21.

3. LES Simulation of Isotropic Decaying Turbulence

In order to validate the solver in the LES mode, the simulation of decaying homogeneous isotropic turbulence is computed and the energy spectra of the flow field are compared with experimental results from Comte-Bellot and Corrsin [6]. Strelets [7] has performed similar computations which were used to calibrate the value of the C_{DES} model constant. In the present work, we are mainly concerned with assessing the impact of numerical dissipation on solution accuracy, since the scheme is only second-order accurate. Therefore, the value of C_{DES} is held constant at 0.65 for all computations, which is the value recommended by Strelets [7]. Artificial dissipation levels are varied by prescribing different values of the dissipation scaling parameter, and by varying the grid resolution. In addition, simulations with and without the turbulence model eddy viscosity are performed to assess the effect of the turbulence model on overall solution accuracy, and to determine whether the the levels of eddy viscosity dominate the artificial dissipation.

The computational domain consists of a cube with periodic boundary conditions. Because no wall regions are present, the DES model operates in the LES mode throughout the domain regardless of grid resolution. Computations are performed on a coarse and a fine grid, which are constructed as unstructured cartesian grids with 32 and 64 hexahedral cells, respectively, in each dimension of the cubic domain.

In order to compare with the experimental values from [6], the flow field in the computational domain must be initialized as a solenoidal field with a prescribed energy spectrum corresponding to that measured at the initial test section in the experiments (up to the cutoff value of the wave number corresponding to the grid size). The initial eddy viscosity field must then be obtained by preconverging the turbulence model with the flow-field held frozen. Once the initialization is complete, the flow field is advanced in time using the implicit time-stepping procedure described above. A time-step of 0.01 is employed, where time is non-dimensionalized as $t = t_o(1.5u'^2)^{1/2}/L$, where L is the box length, and u' represents the initial rms average velocity fluctuation. The resulting flow fields at t = 0.87 and t= 2.0 are postprocessed to obtain the energy spectra, which are then compared with corresponding experimental data.

Figure 1 illustrates the computed spectra on both grids at two time levels for the nominal value of the artificial dissipation scaling factor, i.e. the value generally employed for steady-state calculations in RANS mode. Clearly, the finer scales decay more rapidly than in the experimental values. When the same simulations are performed with the eddy viscosity turned off, little difference in the energy spectra is observed, suggesting that the eddy viscosity values are overwhelmed by the levels of artificial dissipation.

In Figure 2, the same computations are performed with a lower scaling of the artificial dissipation terms (0.25 of the nominal value). Substantially better agreement is observed at all scales, although the finest scales are still dissipated faster than in the experimental results. However, reasonably good agreement is obtained up to k=10 for the fine grid, and both grids agree reasonably well at lower wave numbers. When the eddy viscosity is omitted in these cases, agreement with experiment degrades, particularly at the lower wave numbers where the dissipation is lower than observed experimentally.

4. DES Flow Over a Sphere

The current solver is applied in DES mode to predict the flow around a sphere. A Mach number of 0.2 was prescribed, while the Reynolds number was set to 10^4, corresponding to the sub-critical regime (laminar boundary layer separation), which is similar to the computations performed in [8], which provides a comparative basis for our results. An unstructured mesh of 767,000 vertices is employed, in a cubic computational domain of 100 sphere diameters in total length. At the surface of the sphere, the normal grid spacing is 10^{-4} sphere diameters.

Two different time-steps of 0.1 and 0.05 are used, where the time-step is non-dimensionalized as shown in equation (1). Four multigrid levels are used, and each physical time-step is solved with 25 multigrid cycles, resulting in a two order of magnitude reduction in the residuals. All runs were performed on a cluster of thirty-two 800 MHz Pentium III PCs, for which the convergence of a physical time-step could be achieved in approximately 6 minutes of wall clock time.

This case has been computed in both DES and URANS mode, using the Spalart-Allmaras turbulence model without modification in the latter case. The time history of the drag coefficient is shown in Figure 3 and reveals important differences between URANS and DES. The mean value of the drag coefficient in both cases is close to the experimentally reported value of 0.40 from Schlichting [9]. However, the URANS simulation appears to damp out most of the oscillations present in the DES run, while the DES runs show a very chaotic oscillatory pattern quite similar to the solutions obtained by Constantinescu et al. [8]. Spectral analysis of the time-dependent drag coefficient history reveals a peak corresponding to a Strouhal number of 0.1 which is not in agreement with the values 0.18 to 0.2 reported experimentally [8]. This may be due to an insufficiently long time history sample, since less than three full periods of this frequency are present in our sample.

In Figure 4, the average surface pressure computed using DES is seen to provide superior agreement with experimental results at Re=165,000

reported by Achenbach [10] in the separated region over the URANS results, and are in agreement with the results reported by Constantinescu [8]. The average computed separation angle of 81° in the DES case compares reasonably to experimental vale of 82.5^o .

5. Conclusions and Further Work

This work prepresents initial efforts at developing and validating a fully implicit parallel LES/DES solver based on unstructured meshes. In the near future, we intend to pursue further validation studies on both basic flows using finer grids and time-steps, and more complex geometries such as flow over bluff body components of aerospace vehicles. Efficiency improvement are also under consideration through the use of higher-order time-stepping procedures and Krylov acceleration methods. This work has been supported by AFOSR under the management of Dr. Len Sakell.

References

[1] D. J. Mavriplis and S. Pirzadeh. Large-scale parallel unstructured mesh computations for 3D high-lift analysis. *AIAA Journal of Aircraft*, 36(6):987–998, 1999.

[2] J. Pelaez, D. J. Mavriplis, and O. Kandil. Unsteady analysis of separated aerodynamic flows using an unstructured multigrid algorithm. AIAA Paper 2001-0860, January 2001.

[3] D. J. Mavriplis. Multigrid strategies for viscous flow solvers on anisotropic unstructured meshes. *Journal of Computational Physics*, 145(1):141–165, September 1998.

[4] P. R. Spalart and S. R. Allmaras. A one-equation turbulence model for aerodynamic flows. *La Recherche Aérospatiale*, 1:5–21, 1994.

[5] P. R. Spalart, W-H. Jou, M. Strelets, and S. R. Allmaras. Comments on the feasibility of LES for wings and on a hybrid RANS/LES approach. Paper presented at the First AFOSR International Conference on DNS and LES, Louisiana Tech University, Ruston, Louisiana, August 1997.

[6] G. Comte-Bellot and S. Corrsin. Simple Eulerian time correlation of full- and narrow-band velocity signals in grid generated isotropic turbulence. *Journal of Fluid Mechanics*, 48(2):273–337, 1971.

[7] M. Strelets. Detached eddy simulation of massively separated flows. AIAA Paper 2001-0879, January 2001.

[8] G. S. Constantinescu and K. D. Squires. LES and DES investigations of turbulent flow over a sphere. AIAA Paper 2000-0540, January 2000.

[9] H. Schlichting. *Boundary Layer Theory*. McGraw-Hill, New York, USA, 1979. Seventh Edition.

[10] E. Achenbach. Experiments on the flow past spheres at very high Reynolds numbers. *Journal of Fluid Mechanics*, 54(3):565–575, 1972.

TABLE 1. Computed Strouhal Number for Various Grid Sizes and Time Steps
for RANS Flow over Circular Cylinder

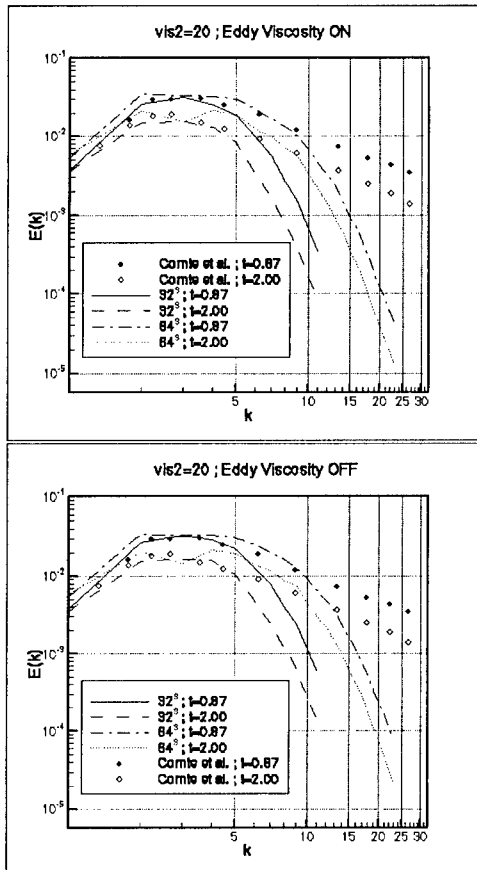| Grid Size (points)	Time Step = 0.5	Time Step = 0.25	Time Step = 0.1
0.252 million	0.19249	0.20304	0.20833
0.631 million	0.19379	0.20408	0.20833

Figure 1. Comparison of Computed and Measured Energy Spectra for Nominal Artificial
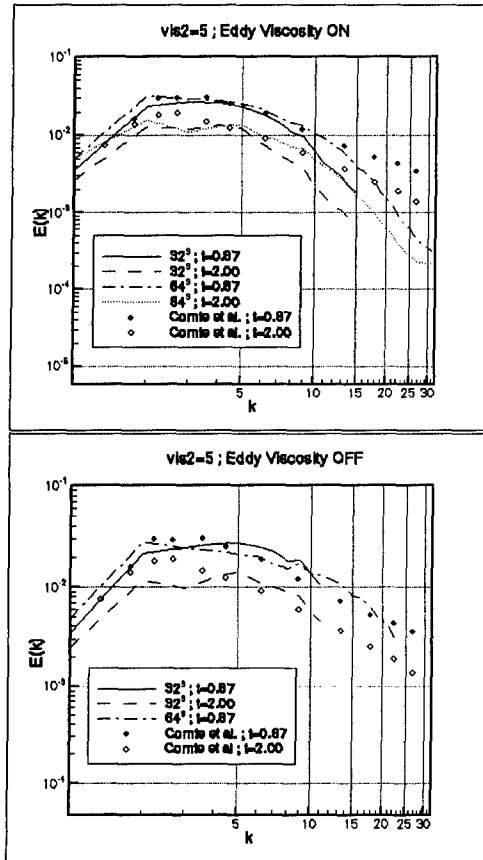Viscosity Levels with Eddy Viscosity (LEFT) and Without Eddy Viscosity (RIGHT)

Figure 2. Comparison of Computed and Measured Energy Spectra for Reduced Artificial Viscosity Levels with Eddy Viscosity (LEFT) and Without Eddy Viscosity (RIGHT)
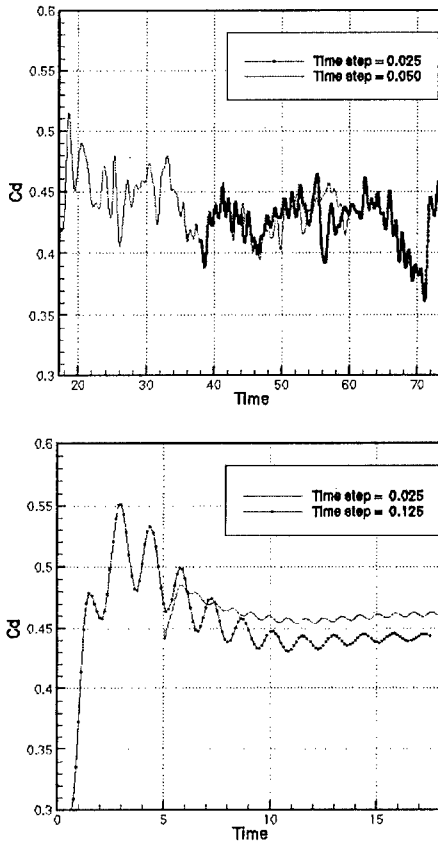
Figure 3.   Comparison of Computed Drag Coefficients for Sphere using DES (LEFT) and URANS (RIGHT)
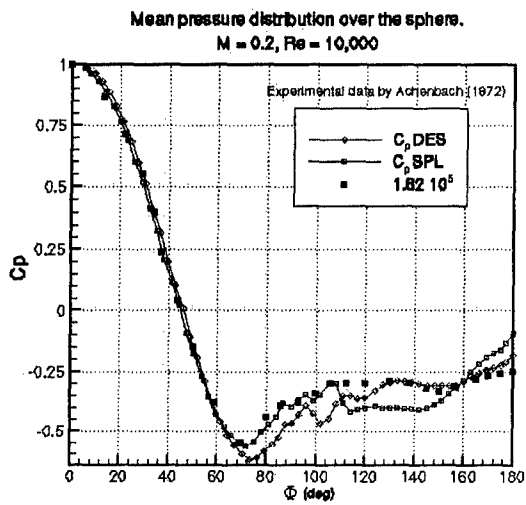
Figure 4. Comparison of Computed Average Surface Pressure Coefficient using DES and URANS versus Experimental Data